A Simple Biophysically Plausible Model for Long Time Constants in Single Neurons

Zoran Tiganj,* Michael E. Hasselmo, and Marc W. Howard

ABSTRACT: Recent work in computational neuroscience and cognitive psychology suggests that a set of cells that decay exponentially could be used to support memory for the time at which events took place. Analytically and through simulations on a biophysical model of an individual neuron, we demonstrate that exponentially decaying firing with a range of time constants up to minutes could be implemented using a simple combination of well-known neural mechanisms. In particular, we consider firing supported by calcium-controlled cation current. When the amount of calcium leaving the cell during an interspike interval is larger than the calcium influx during a spike, the overall decay in calcium concentration can be exponential, resulting in exponential decay of the firing rate. The time constant of the decay can be several orders of magnitude larger than the time constant of calcium clearance, and it could be controlled externally via a variety of biologically plausible ways. The ability to flexibly and rapidly control time constants could enable working memory of temporal history to be generalized to other variables in computing spatial and ordinal representations. © 2014 Wiley Periodicals, Inc.

KEY WORDS: working memory; exponentially decaying firing; persistent firing; calcium-sensitive nonselective cation current; cholinergic modulation

INTRODUCTION

It has been widely accepted that memory of recent events [working memory (Goldman-Rakic, 1995)] is represented through the maintenance of action potential firing rather than through anatomical changes such as synaptic modifications. If that is the case, then neurons that respond to stimulus presentation and then continue to fire after the presentation has ended could be essential for representation of the recent history (Hasselmo and Stern, 2006).

Neurons that continue to fire after the stimulus during the delay period of a memory task have been reported in multiple in vivo studies (Miyashita and Chang, 1988; Funahashi et al., 1989; Miller et al., 1993; Goldman-Rakic, 1996; Miller et al., 1996; Romo et al., 2002). An extensive literature implicates recurrent connections, especially in prefrontal cortex, in sustained firing (Hebb, 1949; Goldman-Rakic, 1995; Compte et al., 2000; Wang, 2001; Wang et al., 2012). However, in vitro work suggests that persistent activity could also be caused by processes intrinsic to single neurons. Persistent firing has been found in slice preparations in a number of brain regions including Layers 2, 3, and 5 of entorhinal cortex (Klink and Alonso, 1997; Egorov et al., 2002; Tahvildari et al., 2007; Jochems et al., 2013), Layer 5 of prefrontal cortex (Haj-Dahmane and Andrade, 1996), lateral amygdala (Egorov et al., 2006), postsubiculum (Yoshida and Hasselmo, 2009), the CA1 region in hippocampus (Knauer et al., 2013) and perirhinal cortex (Navaroli et al., 2011). All of these studies used synaptic blockers to demonstrate that persistent firing can be sustained by individual neurons and does not depend on recurrent connections.

Experimental and theoretical work has been primarily focused on persistent firing with a stable firing frequency. Indeed, neurons can retain the information that a stimulus was presented by maintaining a stable elevated firing rate after the stimulus has ended. However, stable persistent firing cannot carry information about when the stimulus was presented. If a neuron fires at a constant frequency following a stimulus, then one cannot deduce anything about the time when the stimulus occurred or about the duration of the stimulus from its firing rate. Imagine a cognitive experiment in which the same stimulus is repeated to the subject but with different time lags, for example: "TABLE (5s lag) TABLE (5s lag) TABLE (1s lag) TABLE." One ought to be able to recognize that the delay after the third presentation of the stimulus was shorter than the other two. Humans and other animals are able to judge the time at which stimuli were presented over a range of intervals (e.g., Yntema and Trask, 1963; Gibbon, 1977; Roberts et al., 1989; Lejeune and Wearden, 2006; Wearden and Lejeune, 2008; Lewis and Miall, 2009). Stable persistent firing cannot account for this ability.

To account for the memory that can store approximate representation of recent stimulus history, we focus here on neural firing caused by a stimulus that

Department of Psychological and Brain Sciences, Center for Memory and Brain, Boston University, Boston, Massachusetts
*Correspondence to: Zoran Tiganj, Department of Psychological and Brain Sciences, Center for Memory and Brain, Boston University, Boston, Massachusetts. E-mail: zorant@bu.edu
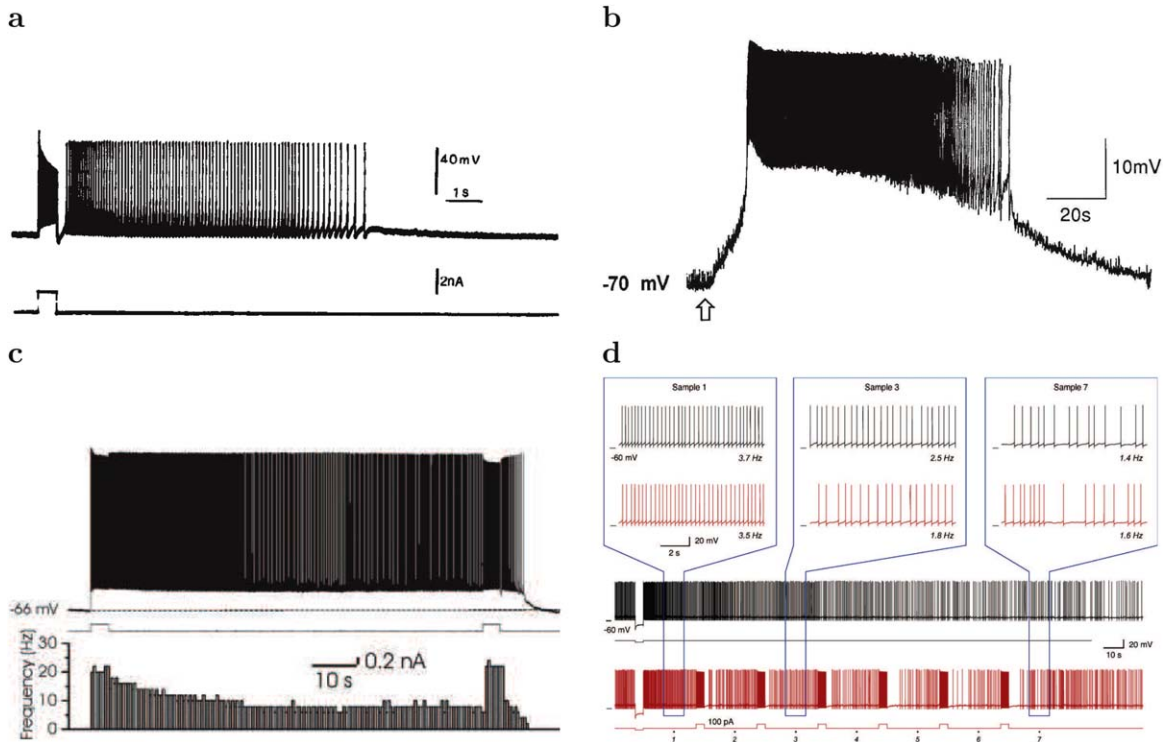
a

b

c

d

FIGURE 1.   Examples of slowly decaying firing rate in slice recordings. (a) Cat Layer 5 Sensorimotor Cortex after application of muscarine-a nonselective agonist of the muscarinic acetylcholine receptor (Schwindt et al., 1988). (b) Acetylcholine-induced depolarization of Layer 5 pyramidal neurons of prefrontal cortex (Haj-Dahmane and Andrade, 1996). The arrow indicates the time of acetylcholine application. (c) Layer 3 of lateral entorhinal cortex in the presence of muscarinic receptor activation (Tahvildari et al., 2007): membrane potential trace on the top, current stimulation trace in the middle and firing rate histogram on the bottom plot. (d) Anterodorsal thalamus (area with a high percentage of head direction cells) after hyperpolarizing stimulus (current trace at the bottom), (Kulkarni et al., 2011). [Color figure can be viewed in the online issue, which is available at wileyonlinelibrary.com.]

then slowly decays. Here, "slowly" is defined with respect to timescale characteristic for intrinsic dynamics of neural mechanisms, much longer than a few hundred milliseconds. Slowly decaying firing has been found in many in vitro studies (see Fig. 1, Schwindt et al., 1988; Haj-Dahmane and Andrade, 1996; Klink and Alonso, 1997; Tahvildari et al., 2007; Winograd et al., 2008; Fransén et al., 2006; Kulkarni et al., 2011; Hyde and Strowbridge, 2012; Yoshida and Hasselmo 2009).

With slowly decaying firing, if the rate of the decay is known, one can reconstruct the time when the stimulus was presented from the firing rate. Many neural models of timing exploit firing rates that change in a lawful way over relatively long periods of time to support behavior (e.g., Gavornik and Shouval, 2011; Simen et al., 2011; Shouval and Gavornik, 2011). However, a single neuron is not able to code the entire stimulus history. In other words, it is not possible to represent a function such as stimulus history with a single scalar value such as firing rate of a neuron. Consider the case in which TABLE is presented multiple times with different delays in between. After the first presentation of TABLE, the firing rate increases to some level and then decreases gradually over time. During the delay between the first and second presentation of TABLE, the firing rate can provide information about how far in the past TABLE was presented.

But now what happens when TABLE is repeated? If the cell is unaffected by the second presentation, but continues to decay, then the second presentation has had no effect and cannot be coded by the neuron. If the neuron responds to the second presentation by going to the same firing rate as immediately after the first presentation and then decays, information about the first presentation is lost. Even if the neuron responds to both presentations in an additive fashion, this is still not sufficient to code for the history. Consider the interval after presentation of the first stimulus. Let us denote the firing rate after 2.5 s have passed as x. After the second stimulus, the firing rate increases to some value higher than immediately after the first presentation of TABLE (due to the additive effects of the two stimulus presentations). If the firing rate eventually decays to zero, it must at some point pass through x; if the decay function is smooth and monotonic, this must happen some time more than 2.5 s after the second presentation of TABLE. But this illustrates the problem of having a single neuron code for a function of stimulus history: the same value x must code for two histories, one history with a single presentation 2.5 s in the past, and another history with two stimulus presentations separated by 5 s in the past.

Shankar and Howard (2012) pointed out that, in principle, complete information about the history of stimulus presentations

can be encoded by a set of exponentially decaying neurons with different time constants. The basic idea is that whereas a single neuron cannot maintain a representation of a stimulus history, a set of many neurons with different time constants can. (This claim can be verified by noting that a set of integrators with different time constants encode the Laplace transform, with real coefficients, of the history leading up to the present moment. Because the Laplace transform is invertible, complete information about the history is still available in the pattern of firing rates across the neurons [see Shankar and Howard, 2012, for details].) This mechanism requires the existence of a set of neurons indexed by s whose firing rates $F(s, t)$ decay exponentially following the stimulus presentations $f(t)$ across time t:

$$\frac{dF(s, t)}{dt} = \alpha(t)[-sF(s, t) + f(t)]. \quad (1)$$

The variable $\alpha(t)$ is a modulatory input to the set of integrators, changing their time constants together as a function of time. Shankar and Howard (2012) provided a description of how this set of leaky integrators, with $\alpha(t) = 1$, can be used to construct a scale-invariant representation of the history of f leading up to the present. (Briefly, the mechanism for extracting the stimulus history from Eq. (1) is essentially a lateral inhibition.) The extracted estimate of history can be used to describe a number of behavioral findings (Shankar and Howard, 2012; Howard and Eichenbaum, 2013; Howard et al., in press). By choosing $\alpha(t)$ judiciously, one can code for functions of variables other than time, including spatial location and ordinal position (Howard et al., 2014). The resulting representation has correlates that resemble those of a variety of neurons in the hippocampus and related regions, including time cells (Pastalkova et al., 2008; MacDonald et al., 2011), boundary vector cells (Lever et al., 2009), place cells (Burgess and O'Keefe, 1996; Mankin et al., 2012), "splitter cells" (Wood et al., 2000), trajectory coding cells, and retrospective coding cells (Frank et al., 2000).

If it could be implemented in neural circuits, Eq. (1) could provide the centerpiece of a model that integrates many aspects of behavior and systems level firing properties of neurons. However, Eq. (1) presents two major challenges for a biological circuit:

1. In order for the model to describe neural firing and behavioral effects up to long time scales, there should be neurons with time constants on the order of that time scale. The time constant of each unit in Eq. (1) is $1/s$.
2. Rapid external control of the time constants of the exponential decay is necessary for an external signal $\alpha(t)$ to modulate Eq. (1).

The primary purpose of this article is to develop a biologically plausible hypothesis for how these two properties could be implemented. Although it is possible that these properties could result from recurrent network connections (see Brody et al., 2003; Major and Tank, 2004, for reviews), we focus here on the possibility that intrinsic currents could be used to implement these two properties.

OVERVIEW

The calcium-activated nonspecific (CAN) cationic current has been demonstrated to be crucial for persistent firing in some in vitro preparations. When CAN current was blocked, or in the absence of calcium, persistent firing did not occur (Egorov et al., 2002; Tahvildari et al., 2008; Yoshida and Hasselmo, 2009; Zhang et al., 2011; Navaroli et al., 2011). Moreover, activation of muscarinic acetylcholine receptors, which leads to CAN current activation, has been shown as necessary for induction of persistent firing in some cases (Egorov et al., 2002; Navaroli et al., 2011; Yoshida et al., 2012). Computational modeling studies have been successful in proposing detailed mechanisms based on the interplay between CAN current and intracellular calcium concentration that could account for stable firing (Fransén et al., 2002; Fransén et al., 2006), linearly growing firing (Durstewitz, 2003), and firing during an interval of learned duration (Shouval and Gavornik, 2011).

Here, we propose a simple model for exponentially decaying after-discharge firing that depends on CAN current. Graded persistent firing (Egorov et al., 2002; Fransén et al., 2006) reflects a perfect integrator with an infinite time constant; the basic idea of this article is to use a similar approach to generate leaky integrators with a range of finite time constants. We show that for a realistic choice of the parameters the firing rate decays approximately exponentially. The time constant of the decay is defined by a set of parameters several of which could be externally tuned, either through synaptic inputs or neuromodulation.

Figure 2 illustrates the proposed feedback loop. After the stimulus presentation, relatively high calcium concentration decays, but also drives the CAN current which depolarizes the cell causing a spike that brings more calcium in the cell effectively prolonging the calcium decay. The rate of the decay is mediated through several mechanisms (Fig. 2a).

Stage 1: Stimulus causes calcium accumulation. We start from the moment when the stimulus that will trigger the exponentially decaying firing is presented (Number 1 in Fig. 2). We assume that the neuron fires in response to the stimulus, leading to an increase of the intracellular calcium level, since during the stimulus calcium enters the cell through voltage-gated calcium channels.

Stage 2: While calcium decays, the CAN current slowly depolarizes the cell causing a spike. After the stimulus presentation has ended the CAN current, which depends on calcium concentration, is relatively strong as calcium concentration is high (Fig. 2b at time $t_0 = 0$). The CAN current depolarizes the cell (Number 2 in Fig. 2) eventually reaching the threshold level so an action potential is fired. During the interspike interval intracellular calcium concentration decays due to the activity of generally present calcium clearance mechanisms, which pump calcium out of the cell or into internal calcium buffers.

Stage 3: During the spike calcium enters the cell. During the action potential voltage-gated calcium channels open again allowing additional calcium influx (Number 3 in Fig. 2) k_{Ca}, which is constant per spike. If this influx is smaller than the amount of calcium pumped out of the cell during the
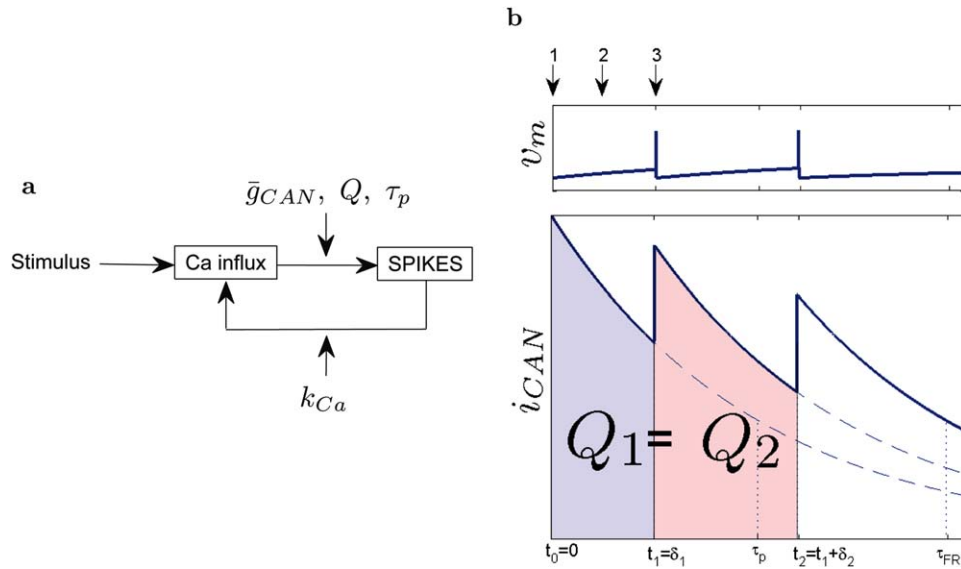
b

FIGURE 2. Illustration of calcium and CAN current-based mechanism for decaying firing. (a) Feedback loop that accounts for decaying firing. Stimulus causes initial accumulation of calcium which then drives the CAN current, which depolarizes the cell and causes a spike. Time needed for the depolarization can be mediated through several mechanisms: time constant of calcium clearance τ_p maximal conductivity of CAN current channels $\bar{g}_{CAN}$ and charge needed to cause each spike Q. The resulting spike causes calcium influx, with the amount defined by k_{Ca}, which closes the loop. (b) Illustration of how calcium influx slows down the overall calcium decay. $i_{CAN}(t)$ is approximately proportional to calcium concentration. When the cell is not firing, calcium con-centration decays, but $i_{CAN}(t)$ still slowly depolarizes the cell (bottom plot) and after it brings enough charge into the cell (Q_1) an action potential is fired (top plot). During the action potential, inward calcium currents cause an increase in calcium concentration. The process repeats. Calcium influx is the same for each spike and is set to be small enough so it does not exceed the value of calcium during the previous spike (i.e., $Ca(t_0)>Ca(t_1)>Ca(t_2)$). We show analytically that the calcium decay is, under the right circumstances, approximately exponential with a time constant much longer than τ_p. [Color figure can be viewed in the online issue, which is available at wileyonlinelibrary.com.]

interspike interval, then the amplitude of the CAN current will be smaller than at the moment when the stimulus presentation has ended at the beginning of the decay (see Fig. 2b).

The CAN current will now continue again to depolarize the cell, but as its new starting amplitude is lower than at the start of the previous depolarization it will take more time for the cell to reach the threshold level, which will result in an increase of the interspike interval. This process will continue iteratively while the CAN current is strong enough to depolarize the cell to the threshold level. Each successive interspike interval will be longer than previous, meaning a firing rate will decay. In the following section, we will analytically show that for a range of parameters, decay of the firing rate is approximately exponential.

MODEL

For analytic tractability, we use a simple integrate and fire model. During interspike intervals, membrane potential as a function of time $v_m(t)$ is modeled as:

$$C_m \frac{dv_m(t)}{dt} = -i_{CAN}(t). \qquad (2)$$

Note that in this extremely simple model i_{CAN} is the only current; there are neither other inputs nor a leak current.

When the membrane potential reaches the threshold level v_t, an action potential is fired and the membrane potential is reset to the reset potential v_r, which is equal to the initial value of the membrane potential $v_m(0)$. Here, C_m is the membrane capacitance, defined by geometric properties of the cell and the specific capacitance of the cell membrane.

Because calcium controls the CAN current, changes of the membrane potential are determined by calcium dynamics. The calcium concentration is assumed to be affected by two mechanisms. (1) Calcium clearance that constantly drives calcium out of the cell with time constant τ_p. (2) A voltage-gated calcium current which contributes meaningfully only during spikes. Calcium clearance is present all the time and calcium influx is present only when the cell is firing an action potential.

We model the change of calcium at each moment as a clearance process that only depends on the instantaneous intracellular calcium concentration $Ca(t)$:

$$\frac{dCa(t)}{dt} = \frac{-Ca(t)}{\tau_p} \Rightarrow Ca(t) = Ca(0)e^{-t/\tau_p}. \qquad (3)$$

this results in exponential decay of the intracellular calcium concentration with the time constant τ_p. As mentioned earlier, we assume that $Ca(0) \gg 0$ due to some external stimulus presentation prior to time zero. For the calcium influx, we assume that each spike causes the same change in calcium

concentration, thus each time when the neuron fires we increase calcium concentration by a fixed amount: k_{Ca}.

Finally, let us describe the relationship between calcium concentration and the CAN current. It will turn out that under certain assumptions the CAN current is approximately proportional to calcium concentration, and depends on the membrane potential v_m. In the form of standard Hodgkin–Huxley model, we can express the CAN current as follows:

$$i_{CAN}(t) = \bar{g}_{CAN} m [v_m(t) - E_{CAN}] \qquad (4)$$

Here, $\bar{g}_{CAN}$ is the maximal value of the ion conductance measured in mho/cm^2, E_{CAN} is the reversal potential of the CAN current ion channels and m is a dimensionless quantity between 0 and 1 that is associated with activation of the CAN current ion channels. Following previous computational work (Traub et al., 1991; Fransén et al., 2002), we let the value of m change from moment to moment according to

$$\frac{dm}{dt} = a\,Ca(t)[1-m] - bm. \qquad (5)$$

where a and b are free parameters. From Eq. (5), we can see that in general the value of m at a particular moment is a function of both time per se as well as the history of calcium concentration.

In the next section, we will show analytically that under appropriate circumstances, the calcium concentration and firing rate decay approximately exponentially. We will derive an expression for this time constant of this exponential decay. In the following section, we will verify the approximation using a computer simulation of the same model.

Analytical Approach

The analytic solution, which results in calcium concentration that decays exponentially, requires that three conditions hold. First, in order for calcium concentration to decay over time, it is essential that the amount of calcium that enters the cell during spikes is smaller than the amount of calcium that clears the cell during an interspike interval. Second, the ratio between an interspike interval and τ_p has to be much lower than one. Third, the CAN current should be proportional to the calcium concentration: $i_{CAN} \propto Ca$. This third condition is met when $a\,Ca(t) \ll b$ and $\frac{1}{a\,Ca(t)+b} \ll \tau_p$. This last condition requires a little bit of discussion.

Starting from Eq. (5), it is easy to show that $m(t) \propto a\,Ca(t)$ holds for a wide range of parameters for the model. If $Ca(t)$ is changing slowly with respect to m, then the stationary state for Eq. (5) can be expressed as: $m_\infty = \frac{a\,Ca}{a\,Ca+b}$. By changing variables to $m' \equiv m - m_\infty$, it is easy to show that the relaxation time to reach that stationary state is $\tau_m = 1/(a\,Ca+b)$. It is evident that for $a\,Ca \ll b$, $m_\infty \propto Ca$. This approximation requires that the effective time constant of Ca is much slower than the relaxation time for m. That is, it requires that $\frac{1}{a\,Ca+b} \ll \tau_p$.

Given that the conductance is proportional to Ca, it remains to be shown that the current is also proportional to Ca. At each

moment, the current will depend not only on the conductance but also by the difference between the membrane voltage and the reversal potential of i_{CAN}, E_{CAN}. However, because there is no leak current, the total charge necessary to cause a spike in a given interspike interval is always the same. This can be estimated from the average current, which can be estimated from the average voltage over the interspike interval $\bar{v}_m$. When these conditions hold, the approximation $i_{CAN} \propto Ca$ emerges from Eq. (4). Simulations to follow will justify these approximations.

We focus on how change of the CAN current amplitude affects the firing rate. Obviously, decaying CAN current will result in decaying firing rate, but we will show that the relationship between CAN current and firing rate is linear. This implies that CAN current that decays exponentially slowly over time will result in exponentially decaying firing rate. To get a further intuition behind the derivations below, one can think that exponential decay of calcium is interrupted by calcium influx every time a spike is generated. Since the time for which each spike prolongs the calcium decay can be well approximated as a linear function of time (under the assumption that new spikes are arriving rapidly with respect to the calcium clearance time constant), the overall calcium decay turns out to be approximately exponential. As overall calcium concentration and the firing rate are coupled, they will decay in a same way. The time constant of the exponential decay depends on the calcium time constant on one side (larger time constant makes the overall decay slower) and strength of CAN current on the other (larger current makes the overall decay slower).

Let us first consider relationship between the CAN current and duration of a single interspike interval. Observe that constant amount of charge, call it Q, is needed to depolarize the cell from the reset potential v_r to the threshold potential v_t: $Q = C_m(v_r - v_t)$. Because there is no leak current, this amount is the same for every interspike interval (see Fig. 2b) and satisfies

$$Q = \int_{t_i}^{t_i+\delta_i} i_{CAN}(t)\,dt \qquad (6)$$

where δ_i is duration of the ith interspike interval.

We consider now two consecutive intervals, such that the first interval starts at $t_0 = 0$. To find the dynamics of the firing rate, we note that Q is the same for both spikes and

$$i_{CAN}(t_0) \int_0^{t_1} e^{-t/\tau_p}\,dt = i_{CAN}(t_1) \int_{t_1}^{t_2} e^{-t/\tau_p}\,dt = Q \qquad (7)$$

where:

$$i_{CAN}(t_1) = i_{CAN}(t_0) e^{-t_1/\tau_p} + k_{CAN} \qquad (8)$$

and

$$k_{CAN} = \bar{g}_{CAN} a\, k_{Ca}(\bar{v}_m - E_{CAN}). \qquad (9)$$

As we will not focus on separately investigating the roles of a, $\bar{v}_m$, and E_{CAN}, for simplicity we gather them in a single constant γ:

$$\gamma \equiv a(\bar{\nu}_m - E_{CAN}) \tag{10}$$

We define $\delta_1 \equiv t_1 - t_0$ and $\delta_2 \equiv t_2 - t_1$. After solving the integrals in Eq. (7) we have

$$e^{-\delta_1/\tau_p} - 1 = \left(e^{-\delta_1/\tau_p} + \frac{k_{CAN}}{i_{CAN}(t_0)} \right) \left(e^{-(\delta_1+\delta_2)/\tau_p} - e^{-\delta_1/\tau_p} \right). \tag{11}$$

Under the assumption $\delta_i/\tau_p \ll 1$, keeping first-order terms, we find $e^{-\delta_i/\tau_p} \approx 1 - \frac{\delta_i}{\tau_p}$. From Eq. (6), it follows that $i_{CAN}(t_0) = \frac{Q}{\delta_1}$. Now we can write the ratio of two consecutive interspike intervals as follows:

$$\frac{\delta_1}{\delta_2} = 1 - \frac{\delta_1}{\tau_p} + \frac{\bar{g}_{CAN} k_{Ca} \gamma}{i_{CAN}(t_0)}. \tag{12}$$

We define firing rate R as a discrete function computed from the interspike intervals δ_i in a following way: $R(t_i) \equiv 1/\delta_{i+1}, \forall i \geq 0$.

$$\frac{R(t_0)}{R(t_1)} = 1 - \delta_1 \left(\frac{1}{\tau_p} - \frac{\bar{g}_{CAN} k_{Ca} \gamma}{Q} \right) \tag{13}$$

Equation (13) implies that the firing rate changes exponentially, with a rate constant that can be computed from Eq. (13). In general, if the firing rate R changes exponentially with time constant τ_R, then for $t_0 = 0$ we can write the ratio $R(t_0)/R(t_1)$ as follows:

$$\frac{R(t_0)}{R(t_1)} = \frac{e^{t_0/\tau_R}}{e^{t_1/\tau_R}} = e^{-\frac{\delta_1}{\tau_R}}. \tag{14}$$

When the interspike interval is small relative to the time constant of the firing rate, we can use a linear approximation: $e^{-\delta_i/\tau_R} \approx 1 - \frac{\delta_i}{\tau_R}$, which gives

$$\frac{R(t_0)}{R(t_1)} = 1 - \frac{\delta_1}{\tau_R}. \tag{15}$$

Now Eqs. (13) and (15) are easily comparable. For the regime where the approximations hold

1. After a depolarizing input that causes spiking the firing rate decays approximately exponentially

$$R(t_i) \approx e^{-t_i/\tau_R} \tag{16}$$

2. The time constant of the decay, τ_R satisfies

$$\frac{1}{\tau_R} = \frac{1}{\tau_p} - \frac{\bar{g}_{CAN} k_{Ca} \gamma}{Q}. \tag{17}$$

Equation (17) conveys a great deal of information. If there is no calcium influx during spikes (if $k_{Ca} = 0$) the time constant of the firing rate decay will be equal to the time constant of the calcium clearance ($\tau_R = \tau_p$). The last term in Eq. (17), $\frac{\bar{g}_{CAN} k_{Ca} \gamma}{Q}$ can not be negative, thus the minimum possible value of the time constant
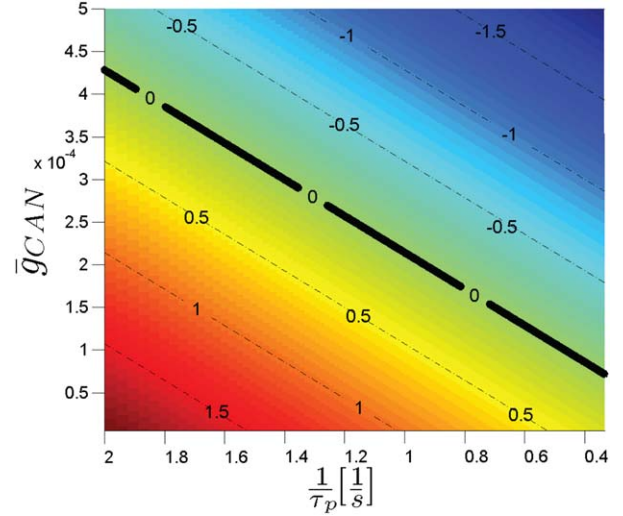
FIGURE 3.   Rate constant of the firing rate (inverse of the time constant $\frac{1}{\tau_R}$) as a function of $\frac{1}{\tau_p}$ (inverse of the calcium clearance time constant) and $\bar{g}_{CAN}$ (maximal conductance of the CAN current ion channels). By controlling any of these two parameters we can theoretically obtain arbitrarily value of the rate constant of the firing rate decay. Notice that for some combinations of the two parameters the firing rate starts to grow—the solid black line indicates the zero values of the rate constant (time constant equal to infinity), below which the firing rate grows exponentially. Similar results would be obtained if $\bar{g}_{CAN}$ was substituted by k_{Ca} (calcium influx during spikes) or Q (the amount of charge required for each spike). [Color figure can be viewed in the online issue, which is available at wileyonlinelibrary.com.]

of firing rate decay τ_R is the value of the time constant of calcium clearance τ_p. Increasing the calcium influx (k_{Ca}), the CAN current maximal conductance ($\bar{g}_{CAN}$) or decreasing the amount of charge required for spike generation (Q) results in increasing the time constant of the firing rate decay τ_R. Figure 3 shows the rate constant $1/\tau_R$ for varying τ_p and $\bar{g}_{CAN}$—similar results would be obtained for k_{Ca} or Q. When the right-hand side of Eq. (17) is equal to zero the time constant is equal to infinity (this value is marked with the black line on Fig. 3). This is an important result; as long as the assumptions used in the derivation hold, there is no upper limit to the time constant of decay.

The findings above provide a means to implement Eq. (1) with long time constants. Because there are several parameters that control the time constant, neurons with different values for any of the parameters on the right-hand side of Eq. (17) will have different time constants. To the extent the values of these parameters can be manipulated rapidly, rapid changes in the time constant are possible as required to implement $\alpha(t)$ in Eq. (1). In the following section, we will perform a set of simulations to confirm that the full model exhibits exponential decay, with a time constant specified by Eq. (17), for a wide range of plausible parameters.

Simulations

We performed a set of simulation, using MATLAB (version R2011a), with the integrate and fire single-compartment model
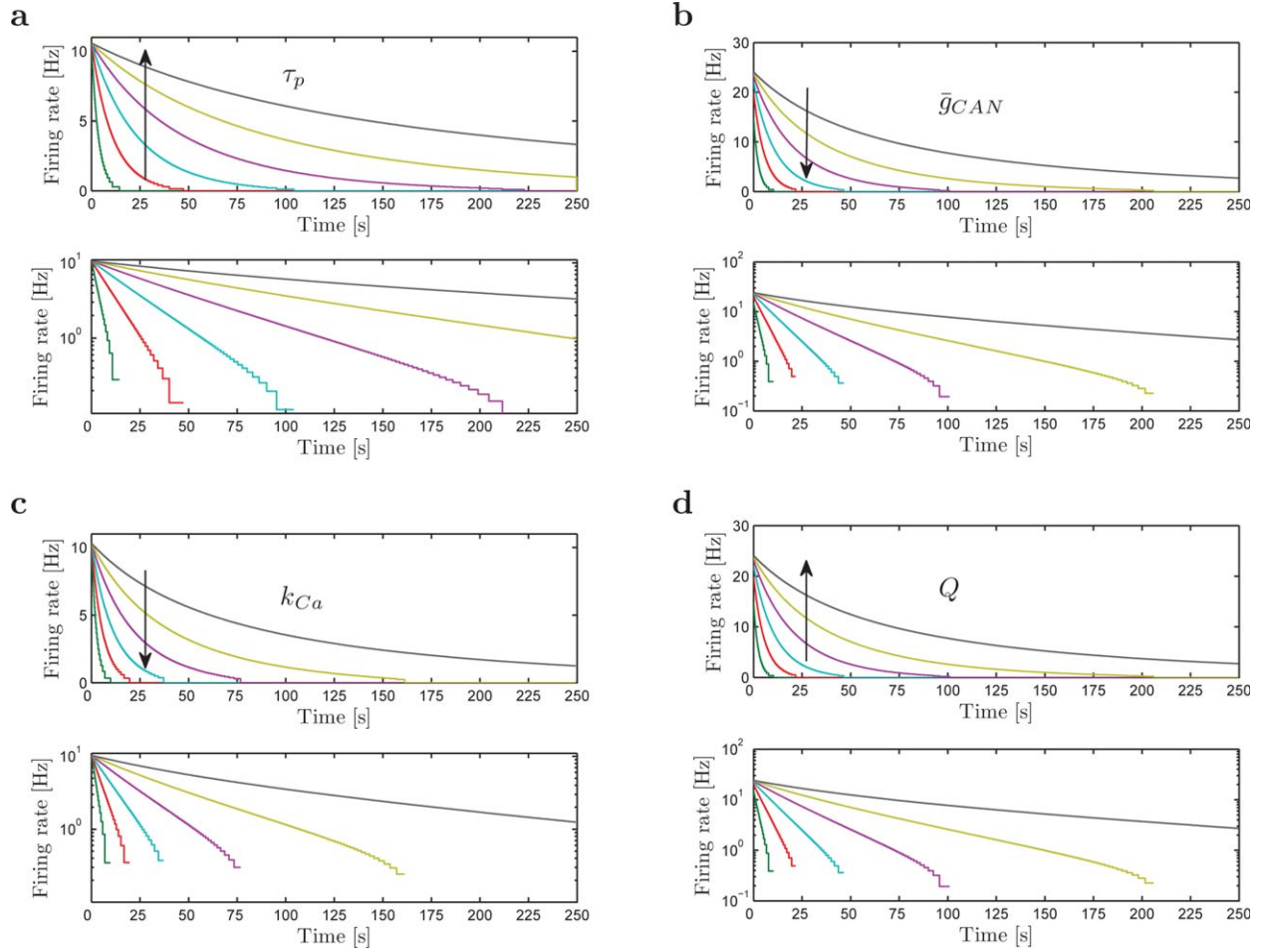
FIGURE 4. Simulated firing rate decays exponentially with various time constant for different values of calcium clearance time constant τ_p, conductivity of the CAN current channels $\bar{g}_{CAN}$, calcium influx during spikes k_{Ca} and the charge required for spike generation Q. Top plot on each of the four figures shows firing rate in linear scale, while bottom plots show firing rate in log scale. Approximately straight lines in the log-plots confirm that the overall decays can be well approximated as exponential. For low firing rates (<1Hz), the decay deviates from exponential due to increased inaccuracy in the time constant estimation. In each plot, the parameter manipulated is displayed. The arrow shows the ordering corresponding to increasing values of the parameter. (a) Influence of τ_p on the firing rate. Following values of τ_p were used: [1.4, 1.9, 2.1, 2.2, 2.25, 2.28]s. (b) Influence of $\bar{g}_{CAN}$ on the firing rate. The following values of $\bar{g}_{CAN}$ were used: $[1.4, 1.9, 2.1, 2.2, 2.25, 2.28]10^{-4}\frac{mho}{cm^2}$. (c) Influence of k_{Ca} on the firing rate. Following values of k_{Ca} were used: [0.5, 1.4, 1.9, 2.1, 2.2, 2.25, 2.28]/25. Calcium concentration is given as unitless such that initial calcium concentration is normalized to value 1. (d) Influence of Q on the firing rate. To change Q we changed specific membrane capacitance c_m, so it took the following values: $1/[0.5, 1.4, 1.9, 2.1, 2.2, 2.25, 2.28]\mu F/cm^2$. [Color figure can be viewed in the online issue, which is available at wileyonlinelibrary.com.]

described above. We used the full biophysical model of the CAN current, as in Eqs. (4) and (5) (Traub et al., 1991; Fransén et al., 2002). Through the simulations we will confirm that the simplifications are reasonable. Additionally, the simulations will allow us to explore the parameter space and closely observe how changing calcium clearance time constant τ_p, calcium influx k_{Ca}, the CAN current maximal conductance $\bar{g}_{CAN}$, or the amount of charge required for spike generation Q affect firing rate time constant τ_R.

Unless otherwise specified, values of the parameters of the model were as follows. Discrete time step was set to 0.1 ms (testing with lower time step did not change the results significantly). Calcium influx during each spike was set to 4% of the initial calcium concentration (presumably corresponding to a calcium microdomain related with the CAN current, not to the overall calcium concentration). The calcium clearance time constant τ_p was set to 1 s, consistent with previous studies. [See e.g., Romani et al. (2013); Sidiropoulou and Poirazi (2012) where τp was set to 1.4 s, Mainen and Sejnowski (1996) where value of 0.2 s was used or Royeck et al. (2008) where two clearance mechanisms were used, one with time constant of 0.1 s and the other with time constant of 1 s.] The value of $\bar{g}_{CAN}$, the maximal value of the CAN current ion conductance which determines the CAN current maximal amplitude was set to 1 $\frac{mho}{cm^2}$. This choice is also supported by results from other studies (e.g., Sidiropoulou and Poirazi, 2012). As in Fransén et al. (2002), parameters a and b from Eq. (5) were set to 0.02 and 1, respectively. We set the spiking threshold $v_t = -40$ mV, the reset potential $v_r = -70$ mV,
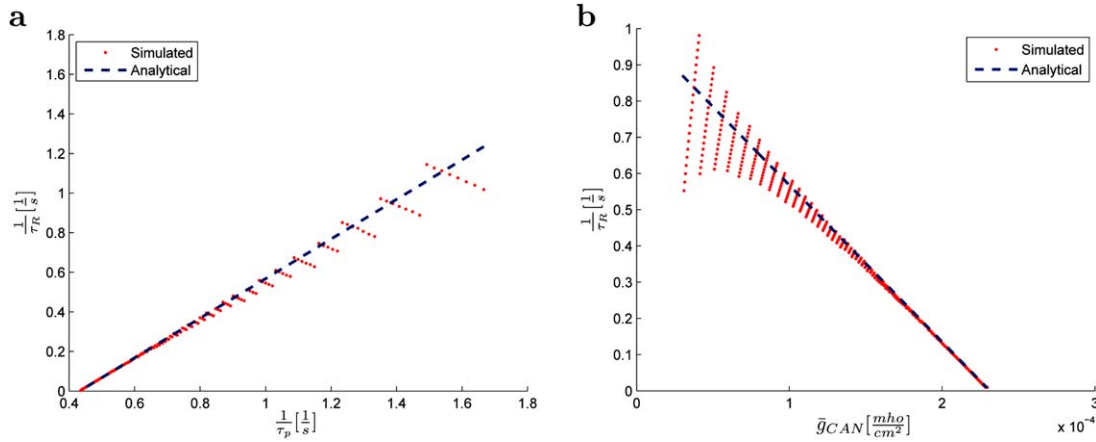
FIGURE 5. Comparison between simulated and analytically obtained time constants. The analytic expression approximates well the simulation over a wide range of parameter values. Inverse of the time constant of the firing rate $1/\tau_R$ is given as a function of: (a) the inverse of the time constant of calcium clearance τ_p and (b) maximal conductance of the CAN current ion channels $\bar{g}_{CAN}$. [Color figure can be viewed in the online issue, which is available at wileyonlinelibrary.com.]

specific membrane capacitance to a value of $1 \frac{\mu F}{cm^2}$, and used a cylindrical compartment with surface of 10^{-4} cm^2. Results to follow will suggest that choice of these values was not critical—the approximations used in the derivation are reasonable for a wide range of parameters.

The four panels of Figure 4 shows the firing rate as a function of time for different values of four parameters on the right-hand side of Eq. (17), τ_p, $\bar{g}_{CAN}$, k_{Ca}, and Q. As the analytical results in the previous section suggest [see Eq. (13)], when observed on a large time scale the overall calcium decay can be well approximated with an exponential function. Figure 4 suggests that by changing any of the four parameters from Eq. (17) (τ_p, $\bar{g}_{CAN}$, k_{Ca}, and Q), we can obtain approximately exponential decay with a wide range of time constants τ_R. By tuning the parameters appropriately, we can achieve a firing rate with virtually any time constant.

To get a sense of the error in the analytic results resulting from the various approximations, we directly compared simulated and analytically computed time constants τ_R for different values of τ_p and $\bar{g}_{CAN}$ (Fig. 5). Analytical results correspond well to the values obtained through the simulations, especially for large time constant τ_R. When τ_R is small, its estimation from the simulations becomes more difficult as only a few spikes are available. Thus, the red dots which denote simulated results on Figures 5a,b oscillate around the blue curves which denote analytical results. This is due primarily to error in the estimation of the time constant as an additional spike becomes available before firing terminates entirely.

DISCUSSION

The aim of the proposed study was to demonstrate that exponentially decaying firing with externally controlled time constants that range up to several minutes is biologically plausible. This result is important to illustrate plausibility of a framework for scale-invariant representation of stimulus history (Shankar and Howard, 2012; Howard et al., 2014). This article provides a proof of concept, rather than a biophysically detailed model. A simple combination of well-known neural mechanisms can account for exponential decay of the firing rate. Variation across cells of any of the quantities on the right-hand side of Eq. (17) would result in a variety of time constants across cells. Rapid manipulation of any of the quantities on the right-hand side of Eq. (17) would enable an external signal to rapidly modulate the time constant, as required to implement time varying $\alpha(t)$ in Eq. (1).

Potential Mechanisms for Rapid External Manipulation of Time Constants

The simplicity of the proposed model allowed us to find an analytical solution for the time constant of the firing rate decay, which pointed out mechanisms to control it. The time constant of the decay depends on the time constant of calcium clearance, the maximum conductivity of the CAN current channels, the amount of calcium influx during spikes and the charge needed to cause each spike. Each of these four parameters could be externally controlled, either through synaptic connections or neuromodulators.

A range of experimental data support a potential role of acetylcholine in regulating the time constants of exponential decay of persistent spiking. Maximal conductivity of the CAN current can be modulated by changing the acetylcholine level (Klink and Alonso, 1997; Egorov et al., 2002; Fransén et al., 2002, 2006; Yoshida and Hasselmo, 2009; Yoshida et al., 2012). Cholinergic modulation will also influence the amount of charge necessary to generate a spike by altering potassium conductances including

the leak potassium current and calcium-sensitive potassium currents (Klink and Alonso, 1997; Fransén et al., 2002, 2006). This functional role of acetylcholine is consistent with data showing that blockade of muscarinic cholinergic receptors causes a reduction of persistent activity during a working memory task (Schon et al., 2005; Hasselmo and Stern, 2006) and blockade of muscarinic receptors impairs learning of conditioning stimuli that must be remembered across a trace interval (Bang and Brown, 2009; Esclassan et al., 2009). The time course of cholinergic modulation depends on how fast the concentration of acetylcholine can change and on the time course of muscarinic receptor activation. It has been shown that the levels of acetylcholine measured by amperometry in cortex can increase and decrease within 1 or 2 s, so the time constant of the change in acetylcholine concentration at the receptor could be on the order of hundreds of milliseconds (e.g., Parikh et al., 2007). It could possibly be faster as the amperometry measurement technique might have time limits. Regarding the time course of muscarinic receptor activation, even though some earlier work showed that its time course to be of the order of seconds in vitro (Hasselmo and Fehlau, 2001; Cole and Nicoll, 1984), in vivo work suggests that it could be faster in vivo (Linster and Hasselmo, 2000).

Any mechanism that can deliver a constant amount of charge per spike into the cell will effectively change the amount of charge necessary to generate a spike. One could imagine a number of simple circuits that might do this in an externally modulated way. For instance, a circuit where the output of an exponentially decaying neuron is connected to the input of some control neuron which fires a burst of spikes each time the exponentially decaying neuron fires a spike and is connected with the input of the exponentially decaying neuron closing the feedback loop. This control neuron will deliver charge to the exponentially decaying neuron each time the exponentially decaying neuron fires. If the number of spikes within each burst of the control neuron is modulated by some control signal then the amount of charge delivered to the exponentially decaying neuron will be controlled by the same signal, consequently controlling the time constant of the decay as well.

The slope of the f-I curve is determined by the amount of charge necessary to generate a spike. Mechanisms that result in change of the slope might be useful for controlling the time constant, as long as they do not perturb the exponential decay. One possible candidate could be dendritic inhibition. This mechanism is presented in a study which combines slice electrophysiology and computational modeling (Mehaffey et al., 2005). The study shows that reduction of a depolarizing afterpotential, arising from active dendritic spike backpropagation, by dendritic inhibition leads to change of the slope of the f-I curve. If it affects the slope of the f-I curve, dendritic inhibition could rapidly change the time constant of a neuron under external control.

Finally, the time constant of calcium clearance τ_p depends on the number and rate of the protein mechanisms that continuously eject calcium ions out of the cell. Selective modulation of either the number or the rate could affect the time constant of calcium clearance.

Experimental Evidence for Gradually Decaying Firing

Recordings in vivo and in vitro have already revealed the existence of persistent firing and slowly decaying firing (see Fig. 1). For slowly decaying firing, the decay is typically fast in the beginning and slower later, roughly resembling the exponential function. In previous studies, slowly decaying firing has not received as much attention as stable persistent firing. While the proposed model can in principle account for stable persistent firing [a time constant of infinity when the right-hand side of Eq. (17)], this is unstable. Previous computational models of stable persistent spiking have proposed an attractor mechanism, based on advanced control of calcium dynamics that could account for this stability (e.g., Durstewitz, 2003; Fransén et al., 2006). Stability around the stable firing rate regime has been obtained using the variance of the intracellular calcium as a control signal (Durstewitz, 2003) and by creating a neutral zone insensitive to small calcium variations (Fransén et al., 2006). Similar mechanisms could account for stable persistent firing in this framework as well.

CONCLUSIONS

Neurons with exponentially decaying firing rates with long time constants that can be externally modulated are computationally very powerful (Shankar and Howard, 2012; Howard et al., 2014). We developed a simple computational mechanism based on known properties that can generate exponentially decaying firing with arbitrarily long time constants. This is a necessary condition for implementing a model for representing temporal history extending over behavioral time scales (Shankar and Howard, 2012). To the extent that the quantities on the right-hand side of Eq. (17) can be externally manipulated, the time constant of exponential decay could be modulated by an external signal. This would allow for the representation of a number of variables other than time, including spatial location and ordinal position (Howard et al., 2014). Systematic experimental investigation of exponential firing in vitro could elucidate the effect of cellular-level parameters on time constants of intrinsic firing. To the extent this computational framework for representing temporal histories is important in brain function, such studies could also inform systems level models of neural function and even behavior (Howard et al., in press).

REFERENCES

Bang S, Brown T. 2009. Perirhinal cortex supports acquired fear of auditory objects. Neurobiol Learn Mem 92:53–62.

Brody CD, Romo R, Kepecs A. 2003. Basic mechanisms for graded persistent activity: Discrete attractors, continuous attractors, and dynamic representations. Curr Opin Neurobiol 13:204–211.

Burgess N, O'Keefe J. 1996. Neuronal computations underlying the firing of place cells and their role in navigation. Hippocampus 6: 749–762.

Cole AE, Nicoll RA. 1984. Characterization of a slow cholinergic post-synaptic potential recorded in vitro from rat hippocampal pyramidal cells. J Physiol 352:173–188.

Compte A, Brunel N, Goldman-Rakic PS, Wang XJ. 2000. Synaptic mechanisms and network dynamics underlying spatial working memory in a cortical network model. Cereb Cortex 10:910–923.

Durstewitz D. 2003. Self-organizing neural integrator predicts interval times through climbing activity. J Neurosci 23:5342–5353.

Egorov AV, Hamam BN, Fransén E, Hasselmo ME, Alonso AA. 2002. Graded persistent activity in entorhinal cortex neurons. Nature 420:173–178.

Egorov AV, Unsicker K, von Bohlen und HO. 2006. Muscarinic control of graded persistent activity in lateral amygdala neurons. Eur J Neurosci 24:3183–3194.

Esclassan F, Coutureau E, Di Scala G, Marchand A. 2009. A cholinergic-dependent role for the entorhinal cortex in trace fear conditioning. J Neurosci 29:8087–8093.

Frank LM, Brown EN, Wilson M. 2000. Trajectory encoding in the hippocampus and entorhinal cortex. Neuron 27:169–178.

Fransén E, Alonso AA, Hasselmo ME. 2002. Simulations of the role of the muscarinic-activated calcium-sensitive nonspecific cation current INCM in entorhinal neuronal activity during delayed matching tasks. J Neurosci 22:1081–1097.

Fransén E, Tahvildari B, Egorov AV, Hasselmo ME, Alonso AA. 2006. Mechanism of graded persistent cellular activity of entorhinal cortex layer V neurons. Neuron 49:735–746.

Funahashi S, Bruce C, Goldmanrakic PS. 1989. Mnemonic coding of visual space in the monkeys dorsolateral prefrontal cortex. J Neurophysiol 61:331–349.

Gavornik JP, Shouval HZ. 2011. A network of spiking neurons that can represent interval timing: Mean field analysis. J Comput Neurosci 30:501–513.

Gibbon J. 1977. Scalar expectancy theory and Weber's law in animal timing. Psychol Rev 84:279–325.

Goldman-Rakic PS. 1995. Cellular basis of working memory. Neuron 14:477–485.

Goldman-Rakic PS. 1996. Regional and cellular fractionation of working memory. Proc Natl Acad Sci USA 93:13473–13480.

Haj-Dahmane S, Andrade R. 1996. Muscarinic activation of a voltage-dependent cation nonselective current in rat association cortex. J Neurosci 16:3848–3861.

Hasselmo ME, Fehlau BP. 2001. Differences in time course of ACh and GABA modulation of excitatory synaptic potentials in slices of rat hippocampus. J Neurophysiol 86:1792–1802.

Hasselmo ME, Stern CE. 2006. Mechanisms underlying working memory for novel information. Trends Cogn Sci 10:487–493.

Hebb DO. 1949. Organization of Behavior. New York: Wiley.

Howard MW, Eichenbaum H. 2013. The hippocampus, time, and memory across scales. J Exp Psychol: Gen 142:1211–13230.

Howard MW, MacDonald CJ, Tiganj Z, Shankar KH, Du Q, Eichenbaum H, Hasselmo ME. 2014. A unified mathematical framework for coding time, space, and sequences in the medial temporal lobe. J Neurosci 34:4692–4707.

Howard MW, Shankar KH, Aue W, Criss AH. A quantitative model of time in episodic memory. Psychol Rev (in press).

Hyde RA, Strowbridge BW. 2012. Mnemonic representations of transient stimuli and temporal sequences in the rodent hippocampus in vitro. Nat Neurosci 15:1430–1438.

Jochems A, Reboreda A, Hasselmo ME, Yoshida M. 2013. Cholinergic receptor activation supports persistent firing in layer {III} neurons in the medial entorhinal cortex. Behav Brain Res 254:108–115.

Klink R, Alonso A. 1997. Muscarinic modulation of the oscillatory and repetitive firing properties of entorhinal cortex layer II neurons. J Neurophysiol 77:1813–1828.

Knauer B, Jochems A, Valero-Aracama M, Yoshida M. 2013. Long-lasting intrinsic persistent firing in rat CA1 pyramidal cells: A possible mechanism for active maintenance of memory. Hippocampus 23:820–831.

Kulkarni M, Zhang K, Kirkwood A. 2011. Single-cell persistent activity in anterodorsal thalamus. Neurosci Lett 498:179–184.

Lejeune H, Wearden JH. 2006. Scalar properties in animal timing: Conformity and violations. Q J Exp Psychol 59:1875–1908.

Lever C, Burton S, Jeewajee A, O'Keefe J, Burgess N. 2009. Boundary vector cells in the subiculum of the hippocampal formation. J Neurosci 29:9771–9777.

Lewis PA, Miall RC. 2009. The precision of temporal judgement: Milliseconds, many minutes, and beyond. Philos Trans R Soc Lond B 364:1897–1905.

Linster C, Hasselmo ME. 2000. Neural activity in the horizontal limb of the diagonal band of Broca can be modulated by electrical stimulation of the olfactory bulb and cortex in rats. Neurosci Lett 282: 157–160.

MacDonald CJ, Lepage KQ, Eden UT, Eichenbaum H. 2011. Hippocampal "time cells" bridge the gap in memory for discontiguous events. Neuron 71:737–749.

Mainen ZF, Sejnowski TJ. 1996. Influence of dendritic structure on firing pattern in model neocortical neurons. Nature 382:363–366.

Major G, Tank D. 2004. Persistent neural activity: Prevalence and mechanisms. Curr Opin Neurobiol 14:675–684.

Mankin EA, Sparks FT, Slayyeh B, Sutherland RJ, Leutgeb S, Leutgeb JK. 2012. Neuronal code for extended time in the hippocampus. Proc Natl Acad Sci 109:19462–19467.

Mehaffey W, Doiron B, Maler L, Turner R. 2005. Deterministic multiplicative gain control with active dendrites. J Neurosci 25:9968–9977.

Miller EK, Li L, Desimone R. 1993. Activity of neurons in anterior inferior temporal cortex during a short-term-memory task. J Neurosci 13:1460–1478.

Miller EK, Erickson CA, Desimone R. 1996. Neural mechanisms of visual working memory in prefrontal cortex of the macaque. J Neurosci 16:5154–5167.

Miyashita Y, Chang HS. 1988. Neuronal correlate of pictorial short-term memory in the primate temporal cortex. Nature 331:68–70.

Navaroli VL, Zhao Y, Boguszewski P, Brown TH. 2011. Muscarinic receptor activation enables persistent firing in pyramidal neurons from superficial layers of dorsal perirhinal cortex. Hippocampus 22:1392–1404.

Parikh V, Kozak R, Martinez V, Sarter M. 2007. Prefrontal acetylcholine release controls cue detection on multiple timescales. Neuron 56:141–154.

Pastalkova E, Itskov V, Amarasingham A, Buzsaki G. 2008. Internally generated cell assembly sequences in the rat hippocampus. Science 321:1322–1327.

Roberts WA, Cheng K, Cohen JS. 1989. Timing light and tone signals in pigeons. J Exp Psychol Anim Behav Process 15:23–35.

Romani A, Marchetti C, Bianchi D, Leinekugel X, Poirazi P, Migliore M, Marie H. 2013. Computational modeling of the effects of amyloid-beta on release probability at hippocampal synapses. Front Comput Neurosci 7:1.

Romo R, Hernandez A, Lemus L, Zainos A, Brody CD. 2002. Neuronal correlates of decision-making in secondary somatosensory cortex. Nat Neurosci 5:1217–1225.

Royeck M, Horstmann MT, Remy S, Reitze M, Yaari Y, Beck H. 2008. Role of axonal NaV1.6 sodium channels in action potential initiation of CA1 pyramidal neurons. J Neurophysiol 100:2361–2380.

Schon K, Atri A, Hasselmo M, Tricarico M, LoPresti M, Stern C. 2005 Scopolamine reduces persistent activity related to long-term

encoding in the parahippocampal gyrus during delayed matching in humans. J Neurosci 25:9112–9123.

Schwindt PC, Spain WJ, Foehring RC, Chubb MC, Crill WE. 1988. Slow conductances in neurons from cat sensorimotor cortex in vitro and their role in slow excitability changes. J Neurophysiol 59:450–467.

Shankar KH, Howard MW. 2012. A scale-invariant representation of time. Neural Comput 24:134–193.

Shouval HZ, Gavornik JP. 2011. A single spiking neuron that can represent interval timing: Analysis, plasticity and multi-stability. J Comput Neurosci 30:489–499.

Sidiropoulou K, Poirazi P. 2012. Predictive features of persistent activity emergence in regular spiking and intrinsic bursting model neurons. PLoS Comput Biol 8:e1002489+.

Simen P, Balci F, deSouza L, Cohen JD, Holmes P. 2011. A model of interval timing by neural integration. J Neurosci 31:9238–9253.

Tahvildari B, Fransén E, Alonso AA, Hasselmo ME. 2007. Switching between "On" and "Off" states of persistent activity in lateral entorhinal layer III neurons. Hippocampus 17:257–263.

Tahvildari B, Alonso AA, Bourque CW. 2008. Ionic basis of ON and OFF persistent activity in layer III lateral entorhinal cortical principal neurons. J Neurophysiol 99:2006–2011.

Traub RD, Wong RKS, Miles R, Michelson H. 1991. A model of a CA3 pyramidal neuron incorporating voltage-clamp data on intrinsic conductances. J Neurophysiol 66:635–650.

Wang M, Yang Y, Wang C-J, Gamo NJ, Jin LE, Mazer JA, Morrison JH, Wang XJ, Arnsten AF. (2012). NMDA receptors subserve persistent neuronal firing during working memory in dorsolateral prefrontal cortex. Neuron 77:736–749.

Wang X. 2001. Synaptic reverberation underlying mnemonic persistent activity. Trends Neurosci 24:455–463.

Wearden JH, Lejeune H. 2008. Scalar properties in human timing: Conformity and violations. Q J Exp Psychol 61:569–587.

Winograd M, Destexhe A, Sanchez-Vives MV. 2008. Hyperpolarization-activated graded persistent activity in the prefrontal cortex. Proc Natl Acad Sci USA 105:7298–7303.

Wood ER, Dudchenko PA, Robitsek RJ, Eichenbaum H. 2000. Hippocampal neurons encode information about different types of memory episodes occurring in the same location. Neuron 27:623–633.

Yntema DB, Trask FP. 1963. Recall as a search process. J Verbal Learning Verbal Behav 2:65–74.

Yoshida M, Hasselmo ME. 2009. Persistent firing supported by an intrinsic cellular mechanism in a component of the head direction system. J Neurosci 29:4945–4952.

Yoshida M, Knauer B, Jochems A. 2012. Cholinergic modulation of the CAN current may adjust neural dynamics for active memory maintenance, spatial navigation and time-compressed replay. Front Neural Circuits, 6:10.

Zhang Z, Reboreda A, Alonso AA, Barker PA, Séguéla P. 2011. TRPC channels underlie cholinergic plateau potentials and persistent activity in entorhinal cortex. Hippocampus 21:386–397.